HHS Public Access

Author manuscript

Int J Radiat Oncol Biol Phys. Author manuscript; available in PMC 2018 March 01.

Published in final edited form as:

Int J Radiat Oncol Biol Phys. 2017 March 01; 97(3): 596–605. doi:10.1016/j.ijrobp.2016.11.004.

Direct comparison of respiration-correlated four-dimensional magnetic resonance imaging (4DMRI) reconstructed based on concurrent internal navigator and external bellows

Guang Li, Ph.D[*,1], **Jie Wei, Ph.D**[2,#], **Devin Olek, M.S**[1,#], **Mo Kadbi, Ph.D**[3], **Neelam Tyagi, Ph.D**[1], **Kristen Zakian, Ph.D**[1], **James Mechalakos, Ph.D**[1], **Joseph O Deasy, Ph.D**[1], and **Margie Hunt, M.S**[1]

[1]Department of Medical Physics, Memorial Sloan Kettering Cancer Center, New York, NY

[2]Department of Computer Science, City College of New York, New York, NY

[3]Philips Healthcare, Cleveland, OH

Abstract

Purpose—To compare the image quality of amplitude-binned four-dimensional magnetic resonance imaging (4DMRI) reconstructed using two concurrent respiratory (navigator and bellows) waveforms.

Methods and Materials—A prospective, respiratory-correlated 4DMRI scanning program was employed to acquire T2-weighted single-breath 4DMRI image using an internal navigator and external bellows. After 10-second training of a surrogate signal, 2D MRI image acquisition was triggered at a level (bin) and anatomic location (slice) until the bin-slice table was filled for 4DMRI reconstruction. The bellows signal was always collected, even when the navigator trigger was used, to retrospectively reconstruct a bellows-rebinned 4DMRI. Ten volunteers participated in this IRB-approved 4DMRI study and four scans were acquired for each subject, including coronal and sagittal scans triggered by either navigator or bellows, and six 4DMRI images (navigator-triggered, bellows-rebinned, and bellows-triggered) were reconstructed. The simultaneously acquired waveforms and resulting 4DMRI image quality were compared using signal correlation, bin/phase shift, and binning motion artifacts. The consecutive bellows-triggered 4DMRI was used for indirect comparison.

Results—Correlation coefficients between navigator and bellows signals were found to be patient-specific and inhalation-/exhalation-dependent, ranging from 0.1 to 0.9, due to breathing irregularities (>50% scans) and commonly-observed bin/phase shifts (−1.1±0.6 bin) in both 1D waveforms and diaphragm motion extracted from 4D images. The navigator-triggered 4DMRI

[*]Corresponding Author: Guang Li, PhD, DABR, Associate Attending Physicist, Department of Medical Physics, Memorial Sloan-Kettering Cancer Center, 1275 York Avenue, New York, NY 10065, Tel: 212-639-2891, lig2@mskcc.org.
[#]These two authors have equal contribution to this study.

Disclosure: This work is in collaboration with Philips Healthcare.

contains much fewer binning motion artifacts at the diaphragm than bellows-rebinned and bellows-triggered 4DMRI. Coronal scans are faster than sagittal scans due to fewer slices and higher achievable acceleration factors.

Conclusion—Navigator-triggered 4DMRI contains substantially fewer binning motion artifacts than bellows-rebinned and bellows-triggered 4DMRI, primarily due to the deviation of the external from the internal surrogate. This study compares two concurrent surrogates during the same 4DMRI scan and their resulting 4DMRI quality. The navigator-triggered 4DMRI scanning protocol is preferred to the bellows-based, especially the coronal scans, for clinical respiratory motion simulation.

Keywords

Respiratory motion simulation; Magnetic resonance imaging; Image reconstruction; Treatment planning; Motion artifacts

Introduction

A reliable respiratory motion surrogate is essential to produce high-quality respiratory-correlated (RC) four-dimensional (4D) images for motion simulation and assessment in radiotherapy treatment planning (1, 2). Some newly developed respiratory-correlated 4D magnetic resonance imaging (RC-4DMRI) can utilize an internal navigator as a respiratory surrogate for prospective or retrospective binning in 4D image reconstruction (3–5). The navigator is often placed on the right diaphragm, and therefore can directly monitor respiratory motion. Generally, such an internal surrogate would be superior to an external surrogate; however, there is a lack of direct evidence depicting the difference between internal and external surrogates in relationship to their resulting 4D images. A study using two simultaneous surrogates can provide a better understanding of respiratory motion as well as clinical guidance on the selection of a motion surrogate and scan conditions. Therefore, it is worthwhile to characterize the differences, advantages, and limitations of these surrogates in 4D simulations.

Since respiratory-correlated 4DCT was first reported around 2003 (6–8), three respiratory motion surrogates have been utilized: i) a real-time position management (RPM) system based on abdominal surface motion, ii) a tension sensor-based bellows to detect changes in abdominal circumference, and iii) conventional spirometry to measure respiratory tidal volume (1). These local point-, line- and volume-based surrogates may suffer from advanced or delayed responses due to soft tissue elasticity, breathing hysteresis non-linearity, and complex location-dependent motion distribution in the anterior-posterior (AP) and superior-inferior (SI) directions. A comprehensive respiratory motion surrogate has been reported using optical surface imaging to monitor the entire torso and quantify both tidal volume and its spatial distribution between the thorax and abdomen, so that SI motion can be decoupled from AP motion, serving as an accurate SI motion surrogate (9–11). Recently, internal anatomical motions extracted from scout-like scans were used to reconstruct 4DCT as a better alternative to an external surrogate (12). In 4DMRI studies, various respiratory surrogates have been examined, including a) in-image surrogates from body area in axial slices (13) or mutual information (14), b) external surrogates from RPM (13) or bellows

(15–17), c) self-navigating in radial acquisition (18), and d) internal surrogates using a navigator placed on the diaphragm (3–5, 15). The diaphragm-based navigator echo probes the most relevant SI diaphragm motion, and therefore should serve as the most direct respiratory motion surrogate. So far, comparisons between these surrogates have been indirect based on two consecutive scans (15, 19, 20), in which breathing irregularities may complicate result interpretation. Direct comparison of navigator and bellows waveforms were reported (21) during respiratory-gated 3D MRI acquisition, rather than RC-4DMRI acquisition.

In the current study, we investigated a T2-weighted (T2W) RC-4DMRI (or 4DMRI) method using an internal navigator, external bellows, or both, as respiratory surrogates. For prospective navigator-triggered 4DMRI acquisitions, a simultaneous bellows signal waveform was acquired to reconstruct bellows-rebinned 4DMRI retrospectively, allowing a direct comparison of their image quality. Reported here are the similarities and differences between the two surrogates and resulting 4DMRI images of ten volunteers under an IRB-approved protocol. Finally, preferences in choosing the best surrogate and scan orientation were recommended for radiotherapy treatment planning.

Methods and Materials

Ten healthy volunteers (five male and five female) were recruited in this study under an IRB-approved protocol, and four prospective 4DMRI scans (triggers: navigator/ bellows; scans: coronal/sagittal) were acquired. A 10-second training waveform was acquired for prospective amplitude-binned 4DMRI image acquisition and reconstructed. Two bellows-rebinned 4DMRI (coronal and sagittal) were retrospectively reconstructed from the two navigator-triggered 4DMRI images using the simultaneous bellows signal for direct comparison. Two separated bellows-triggered 4DMRI images were used for indirect comparison. Therefore, a total of six amplitude-binned 4DMRI images were reconstructed for each volunteer, as shown in Figure 1A.

4DMRI scanning protocol and acquisition conditions

A T2W prospective 4DMRI scan protocol was utilized on a 3T MRI scanner (Ingenia, Philips Healthcare, The Netherlands) (5). The pulse sequence is a single-shot, turbo spin echo with the following scan parameters: TE/TR=80/5000–7000ms, flip angle=90°; SENSE (parallel imaging) factor of 2 (coronal), and a half scan (complex conjugation approximation) factor of 0.7. The pixel bandwidth was ~430–470Hz and the acquisition time per slice was 0.5–0.7s. The scan field of view was subject-dependent, approximately $370\times240\times420mm^3$, covering the thorax and upper abdomen. The voxel size was $2\times2\times5mm^3$, with a 2.5mm gap between slices. The numbers of slices were 31 (coronal) and 49 (sagittal) on average.

The navigator (a small MRI scanning window: 6cm long in the SI direction and 3cm wide) was set on the right diaphragm dome, while the bellows (an airbag with a pressure sensor) was placed on the upper abdomen about 5–10cm from the xiphoid process of the sternum under a tightened VELCRO cloth band around the abdomen. For all navigator-triggered 4DMRI scans, the bellows signals were simultaneously acquired.

Prospective and retrospective 4DMRI reconstruction

The 4DMRI images were reconstructed with five amplitude levels (bins) on inhalation and five on exhalation, as shown in Figure 1B. Therefore the ten bins covered six amplitude levels while separating inhalation and exhalation (5). The prospective scan planned to fill a bin-slice table to cover the temporal and spatial dimensions of an 4DMRI, from anterior to posterior in the coronal scans and from left to right in the sagittal scans. Due to breathing irregularities, such as baseline drift or amplitude reduction, the elements at full inhalation or exhalation in the bin-slice table may become difficult, prolonging the acquisition.

To reconstruct bellows-rebinned 4DMRI image, the bin-slice table of an existing navigator-triggered 4DMRI was reassigned using the synchronized bellows waveform, which was downsampled to match navigator frequency of 25Hz from its original 497Hz. Because of the surrogate difference, some bellows bins could contain multiple image slices, while others might have none. For multi-slice bins, a single slice was randomly selected. For empty bins, linear interpolation of the nearest eight neighbors in the bin-slice table was performed. The current scanning software does not permit navigator echoes when using bellows trigger, and therefore navigator-rebinned 4DMRI was not performed.

Data analysis for two concurrent 1D breathing traces

The simultaneous navigator and bellows waveforms were analyzed to assess their correlation and non-linearity. A navigator vs. bellows graph (SI vs. AP motion) was plotted to demonstrate their motion relationship, while their correlations in inhalation and exhalation were calculated for quantification. The motion levels (bins) of the two simultaneous waveforms was analyzed to depict the quality difference in the binning process, since by definition a well-regulated bin width should suggest fewer motion artifacts in the 4DMRI.

Image analysis for two 4DMRI data sets reconstructed using two concurrent surrogates

The six sets of the 4DMRI images per volunteer were evaluated visually using the right and left diaphragm domes as the anatomic landmarks. The motion trajectories of the right and left diaphragmatic domes were tracked through the breathing cycle, producing two trajectories for each 4DMRI and 12 trajectories for each volunteer. The binning artifacts (irregular edges) in the axial view were visually evaluated at both diaphragms. A cross-correlation analysis between the different motion trajectories was performed and the resulting phase (bin) shift was analyzed. The scan durations of the four primary prospective 4DMRI (100% and 95% completion of the bin-slice acquisition) were analyzed to evaluate the clinical viability based on surrogate selection (navigator vs. bellows) and scan direction (coronal vs. sagittal).

Results

Comparison between internal navigator and external bellows waveforms

Figure 2 illustrates simultaneous navigator and bellows waveforms from a regular breather (volunteer 1) and an irregular breather (volunteer 6). When irregular breathing occurs, the navigator and bellows waveforms have little resemblance to each other, especially the full-exhalation baseline (Figures 2C and 2D), causing differences in binning results. Overall,

more than half of the 20 prospective scans contain severe irregularities. Figure 2E depicts the average number of images per slice in the 10 respiratory bins after bellows rebinning using navigator-triggered 4DMRI image slices. Bins near full-inhalation and full-exhalation stages were overfilled due to a relatively long duration, while transitional bins are under-filled, in reference to the guaranteed even distribution (black line) in the prospective navigator binning.

Reconstruction of bellows-rebinned 4DMRI from navigator-triggered 4DMRI

Figure 3 illustrates a direct comparison between two binning processes using the navigator and bellows in a regular and an irregular breather. The navigator levels are grouped tightly in navigator bins, while the bellows levels are more spread in bellows bins, suggesting the motion differences. Moreover, the separation of inhalation and exhalation in the bellows level indicates a non-linear, hysteresis relationship. Figures 3C and 3D illustrate a bin/phase shift between navigator and bellows waveforms and a difference between inhalation and exhalation. Table I tabulates the correlations between the concurrent navigator and bellows data during inhalation and exhalation in the coronal and sagittal scans. The correlation coefficient varies from −0.72 to 0.92 among the 10 volunteers and the correlation is on average higher in inhalation than exhalation.

Comparison of 4DMRI image artifacts for three different binning methods

Figure 4A illustrates the binning artifacts (irregular edges) on the right and left diaphragms among three sets of 4DMRI images. For navigator-triggered 4DMRI, the right diaphragm edge is almost always smooth since the navigator was placed at the right diaphragm. In contrast, the two bellows-binned 4DMRI contain obvious binning artifacts on both diaphragms. This suggests that navigator-binned 4DMRI image quality is superior to bellows-binned 4DMRI. However, the navigator-binned 4DMRI is not perfect: on the left diaphragm artifacts may occur, due to asynchrony of the two diaphragm motions or involvement of cardiac/digestive motion. The directly-acquired coronal and sagittal images within 0.5s demonstrate high-quality 2D T2W images (Figure 4B).

Motion assessment of 4DMRI images from the six sets of 4DMRI images

The SI motion trajectories of the two diaphragm domes as a function of the respiratory bin are displayed in Figure 5. Bin shifts between navigator-triggered and bellows-binned 4DMRI are observed. Figure 6 depicts two distributions of the bin shifts: a systematic lagging shifts in bellows-binned 4DMRI by 0–2.5 bins and a small random shift (<1 bin) between the right and left diaphragm.

Comparison of prospective 4DMRI scanning times

The scanning time for the four primary navigator-triggered and bellows-triggered 4DMRI is listed in Table II. The coronal scans are generally faster (8.7m) than sagittal scans (11.4m) because of fewer numbers of slices and use of SENSE acceleration. Therefore, coronal scans are preferable to sagittal scans in clinical 4D simulation. The efficiency of filling the bin-slice table decreases near the end as waiting time increases: the acquisition of the final 5%

data consumes 20% of the total acquisition time. The time of 95% completion is also listed Table II.

Discussion

Direct comparison of two concurrent respiratory surrogates and the resulting 4DMRI images within one scan are preformed by evaluating correlation, phase shifts, and artifacts. In contrast, indirect comparisons using two consecutive 4DMRI scans (15, 22), breathing irregularities and irreproducibility do not permit a fair comparison.

Direct comparison between navigator 4DMRI and bellows 4DMRI

Although the common consensus on the selection of respiratory surrogate favors using an internal navigator placed on the diaphragm over the external bellows, there has been a lack of direct comparison of their use in RC-4DMRI. This study demonstrates that the use of navigator and bellows waveforms leads to different quality of 4DMRI images. The phase shift observed in the surrogate signals caused a similar bin shift in the 4DMRI image. This direct comparison confirms previous findings based on two consecutive scans (15, 22), providing direct evidence of the superiority of the navigator-triggered 4DMRI because of fewer binning motion artifacts.

Irregular edges in the axial view of RC-4DMRI images represent binning motion artifacts. The bellows-based scans are more susceptible to the artifacts since the bellows is an indirect surrogate of diaphragm motion, unlike the navigator-based scans that use diaphragm motion for binning. The bellows-binned 4DMRI contains more uncertainties than navigator-triggered 4DMRI, including bellows placement uncertainty and external-internal correlation uncertainty. The navigator-triggered 4DMRI may only contain mild motion artifacts at a mobile structure that is distant from the navigator, such as the left diaphragm. It is worthwhile to mention that the navigator signal may be field-strength dependent, but between 3T and 1.5T, navigator echoes are similar to identify the tissue-air interface. Overall, the navigator-triggered 4DMR images are superior. This improved image quality, together with the device-less surrogating approach (12, 13), should be beneficial for radiotherapy target delineation in the clinic.

In the comparisons between the external bellows and internal navigator, only ~50% cases have a correlation coefficient of >0.6 and ~30% have >0.8 (Table I). This is strongly related to the fact that more than half of the breathing waveforms depict severe breathing irregularities, as shown in Figures 2C and 2D (corr=0.2). The nine negative correlations among 40 cases (Table I) suggest that complex breathing patterns may occur with different levels of chest motion involvement. In addition, the uneven distribution for navigator-to-bellows binning (Figure 2E) suggests more artifacts in bellows-binned 4DMRI. Note that the uneven distribution is due to the navigator-bellows relationship, rather the order of rebinning. The motion artifacts observed in the bellow-rebinned 4DMRI images are similar to those of bellows-triggered 4DMRI and 4DCT (23, 24).

The use of concurrent navigator and bellows in respiratory-gated 3D MRI cardiac imaging has been reported (21), and the bellows signal may depend on placement position (21, 25),

due to breathing pattern variations (thoracic vs. abdominal motions) (10, 26, 27). This is the first time that a direct comparison of RC-4DMRI image quality is performed using simultaneous internal and external surrogates.

Limitation of internal navigator and external bellows as organ motion surrogates

The prospective acquisition and reconstruction of 4DMRI using the current software relies on an initial 10-second training period, in which the program establishes the binning levels for the following 10-minute image acquisition. Although this facilitates 4DMRI acquisition, it assumes that the breathing behavior remains unchanged. Therefore, breathing irregularities with greater breathing amplitudes are ignored. This may help to reduce 4DMRI motion artifacts, but it does not faithfully represent the patient's breathing behavior for motion assessment and tumor motion irregularities may be underestimated in the "mythical" breathing cycle.

Thoracic and abdominal motions are often more complex than a pure respiratory motion because of the involvement of other involuntary motions with a different frequency or a random motion, or both. White, et al. (28) found that the left lung moves very differently from the right lung due to the effect of cardiac motion. Feng, et al. (22) reported that pancreatic motion is poorly correlated with diaphragm motion due to the complex abdominal motion. Stemkens, et al. (15) discovered that external surrogates could carry a high-frequency cardiac motion signal, while the pancreatic motion contains a low-frequency digestive motion signal. Organ motions are also deformable; no respiratory surrogate can fully represent organ motion everywhere within a human body. As observed in this study, the left diaphragm that is distant from the navigator may suffer from motion artifacts (Figure 4). This is the fundamental limitation of a RC-4DMRI method. The ultimate solution should be to develop a time-resolved (TR) 4DMRI technique without a motion surrogate, providing patient-specific breathing irregularities cover multiple breathing cycles for 4D treatment planning (29, 30).

Recommendation for clinical use of 4DMRI

Our results indicate that navigator-triggered 4DMRI had much fewer binning artifacts than bellows-binned 4DMRI via direct comparison. Motion artifacts have been reported to cause gross tumor volume (GTV) variation within the breathing cycle of 4DCT in lung cancer by up to 110% (31, 32). By minimizing 4DMRI motion artifacts using the navigator, a reduced GTV uncertainty is expected, especially for tumors that are near the diaphragm with a large motion.

We recommended T2W multi-slice 4DMRI scans in the coronal direction, as the separation of the human torso is less in the AP than lateral directions. Moreover, the coronal scan can take advantage of higher SENSE acceleration as the scan is parallel to the anterior and posterior coil array. Although breath coaching is useful to improve breathing regularity and reduce scan time (17), it may not always be practical in cancer patients and should not be used if it is not used in the treatment. Alternatively, the 4DMRI acquisition time can be reduced by A) introducing a prioritized acquisition procedure starting from extreme respiratory bins first and B) terminating the coronal scan early while sharing or interpolating

posterior slices without moving anatomy. Therefore, greater than 20% of time reduction on average is expected, as the last 5% acquisition consumes 20% of the time (Table II). Furthermore, it is necessary to perform a patient study to evaluate GTV/ITV delineation in comparison with 4DCT, the current standard of care and it is an on-going study under another IRB-approved protocol.

Conclusion

This study provides a direct comparison between navigator-triggered and bellows-binned 4DMRI from the same 4D scan. The navigator-triggered 4DMRI contained significantly less binning motion artifacts than the bellows-binned 4DMRI. Motion hysteresis between the two surrogates was observed and related to the bin/phase shift observed in diaphragm motions. It is our recommendation to use a navigator-triggered coronal scanning protocol for 4DMRI acquisition and further investigation on patients is ongoing prior to the adoption of 4DMRI in radiotherapy clinic.

Acknowledgments

This research is in part supported by the National Institutes of Health (U54 CA137788 and U54 CA132388) and by the MSK Cancer Center Support Grant/Core Grant (P30 CA008748). This work is in part supported by Philips Healthcare through a master research agreement on the collaboration between MSKCC and Philips Healthcare. The authors would like to thank the MRI simulation technologists and all participating volunteers, including KP, GL, AK, JM, SB, CL, LK, PP, NS, NM, under an IRB approved protocol. We are grateful to Mrs. Peter Piechocniski and Paul Booth (MSKCC) for their technical supports and Mr. James Keller (MSKCC) for his help in editing this manuscript.

References

1. Keall PJ, Mageras GS, Balter JM, et al. The management of respiratory motion in radiation oncology report of AAPM Task Group 76. Med Phys. 2006; 33(10):3874–3900. [PubMed: 17089851]
2. Li G, Citrin D, Camphausen K, et al. Advances in 4D medical imaging and 4D radiation therapy. Technol cancer research & treatment. 2008; 7(1):67–81.
3. Hu Y, Caruthers SD, Low DA, et al. Respiratory amplitude guided 4-dimensional magnetic resonance imaging. Int J Radiat Oncol Biol Phys. 2013; 86(1):198–204. [PubMed: 23414769]
4. Du D, Caruthers SD, Glide-Hurst C, et al. High-quality t2-weighted 4-dimensional magnetic resonance imaging for radiation therapy applications. Int J Radiat Oncol Biol Phys. 2015; 92(2): 430–437. [PubMed: 25838186]
5. Krueger S, Nielsen T. Efficient respiratory navigator-based 4D MRI. ISMRM Annual Meeting. 2016; (3949) 23rd.
6. Ford EC, Mageras GS, Yorke E, Ling CC. Respiration-correlated spiral CT: a method of measuring respiratory-induced anatomic motion for radiation treatment planning. Medical physics. 2003; 30(1):88–97. [PubMed: 12557983]
7. Vedam SS, Keall PJ, Kini VR, et al. Acquiring a four-dimensional computed tomography dataset using an external respiratory signal. Physics in medicine and biology. 2003; 48(1):45–62. [PubMed: 12564500]
8. Low DA, Nystrom M, Kalinin E, et al. A method for the reconstruction of four-dimensional synchronized CT scans acquired during free breathing. Med Phys. 2003; 30(6):1254–1263. [PubMed: 12852551]
9. Li G, Huang H, Wei J, et al. Novel spirometry based on optical surface imaging. Med Phys. 2015; 42(4):1690. [PubMed: 25832058]

10. Li G, Wei J, Huang H, et al. Characterization of optical-surface-imaging-based spirometry for respiratory surrogating in radiotherapy. Med Phys. 2016; 43(3):1348. [PubMed: 26936719]
11. Yuan A, Wei J, Gaebler CP, et al. A novel respiratory motion perturbation model adaptable to patient breathing irregularities. Int J Radiat Oncol Biol Phys. 2016 In press.
12. Martin R, Chandler A, Doan D, et al. TU-F-CAMPUS-J-03: Evaluation of a New GE Device-Less Cine 4D-CT. Medical Physics. 2015; 42(6):3645–3645.
13. Cai J, Chang Z, Wang Z, et al. Four-dimensional magnetic resonance imaging (4D-MRI) using image-based respiratory surrogate: a feasibility study. Med Phys. 2011; 38(12):6384–6394. [PubMed: 22149822]
14. Paganelli C, Summers P, Bellomi M, et al. Liver 4DMRI: A retrospective image-based sorting method. Med Phys. 2015; 42(8):4814–4821. [PubMed: 26233208]
15. Stemkens B, Tijssen RH, de Senneville BD, et al. Optimizing 4-dimensional magnetic resonance imaging data sampling for respiratory motion analysis of pancreatic tumors. Int J Radiat Oncol Biol Phys. 2015; 91(3):571–578. [PubMed: 25596109]
16. Catana C. Motion correction options in PET/MRI. Semin Nucl Med. 2015; 45(3):212–223. [PubMed: 25841276]
17. Glide-Hurst CK, Kim JP, To D, et al. Four dimensional magnetic resonance imaging optimization and implementation for magnetic resonance imaging simulation. Pract Radiat Oncol. 2015; 5(6): 433–442. [PubMed: 26419444]
18. Winkelmann S, Schaeffter T, Koehler T, et al. An optimal radial profile order based on the Golden Ratio for time-resolved MRI. IEEE Trans Med Imaging. 2007; 26(1):68–76. [PubMed: 17243585]
19. Peters DC, Shaw JL, Knowles BR, et al. Respiratory bellows-gated late gadolinium enhancement of the left atrium. J Magn Reson Imaging. 2013; 38(5):1210–1214. [PubMed: 23197465]
20. Matsunaga K, Ogasawara G, Tsukano M, et al. Usefulness of the navigator-echo triggering technique for free-breathing three-dimensional magnetic resonance cholangiopancreatography. Magn Reson Imaging. 2013; 31(3):396–400. [PubMed: 23102944]
21. Santelli C, Nezafat R, Goddu B, et al. Respiratory bellows revisited for motion compensation: preliminary experience for cardiovascular MR. Magn Reson Med. 2011; 65(4):1097–1102. [PubMed: 21413074]
22. Feng M, Balter JM, Normolle D, et al. Characterization of pancreatic tumor motion using cine MRI: surrogates for tumor position should be used with caution. Int J Radiat Oncol Biol Phys. 2009; 74(3):884–891. [PubMed: 19395190]
23. Li G, Caraveo M, Wei J, et al. Rapid estimation of 4DCT motion-artifact severity based on 1D breathing-surrogate periodicity. Med Phys. 2014; 41(11):111717. [PubMed: 25370631]
24. Yamamoto T, Langner U, Loo BW Jr, et al. Retrospective analysis of artifacts in four-dimensional CT images of 50 abdominal and thoracic radiotherapy patients. Int J Radiat Oncol Biol Phys. 2008; 72(4):1250–1258. [PubMed: 18823717]
25. Werner R, White B, Handels H, et al. Technical note: development of a tidal volume surrogate that replaces spirometry for physiological breathing monitoring in 4D CT. Medical physics. 2010; 37(2):615–619. [PubMed: 20229870]
26. Li G, Arora NC, Xie H, et al. Quantitative prediction of respiratory tidal volume based on the external torso volume change: a potential volumetric surrogate. Phys Med Biol. 2009; 54(7):1963–1978. [PubMed: 19265201]
27. Li G, Xie H, Ning H, et al. A novel analytical approach to the prediction of respiratory diaphragm motion based on external torso volume change. Phys Med Biol. 2009; 54(13):4113–4130. [PubMed: 19521009]
28. White B, Zhao T, Lamb J, et al. Distribution of lung tissue hysteresis during free breathing. Med phys. 2013; 40(4):043501. [PubMed: 23556925]
29. Tryggestad E, Flammang A, Hales R, et al. 4D tumor centroid tracking using orthogonal 2D dynamic MRI: implications for radiotherapy planning. Med Phys. 2013; 40(9):091712. [PubMed: 24007145]
30. Li, G., J, W., Zakian, K., et al. The framework of establishing super-resolution time-resolved 4DMRI for 4D treatment planning. AAPM: American Associates of Physicists in Medicine; Washingtom DC: 2016.

31. Persson GF, Nygaard DE, Af Rosenschold PM, et al. Artifacts in conventional computed tomography (CT) and free breathing four-dimensional CT induce uncertainty in gross tumor volume determination. Int J Radiat Oncol Biol Phys. 2011; 80(5):1573–1580. [PubMed: 21163584]

32. Li G, Cohen P, Xie H, et al. A novel four-dimensional radiotherapy planning strategy from a tumor-tracking beam's eye view. Phys Med Biol. 2012; 57(22):7579–7598. [PubMed: 23103415]

Summary

This study presents direct comparison of two concurrent respiratory surrogates: internal navigator and external bellows, and their corresponding 4DMRI image quality. Sixty 4DMRI images in ten volunteers were reconstructed and compared. We found that phase shift is common in the concurrent 1D waveforms and motions extracted from 4DMRI images. Navigator-triggered 4DMRI image quality is far superior. This study provides better understanding of external-internal motion relationship, as well as potential use of 4DMRI in replacing 4DCT.

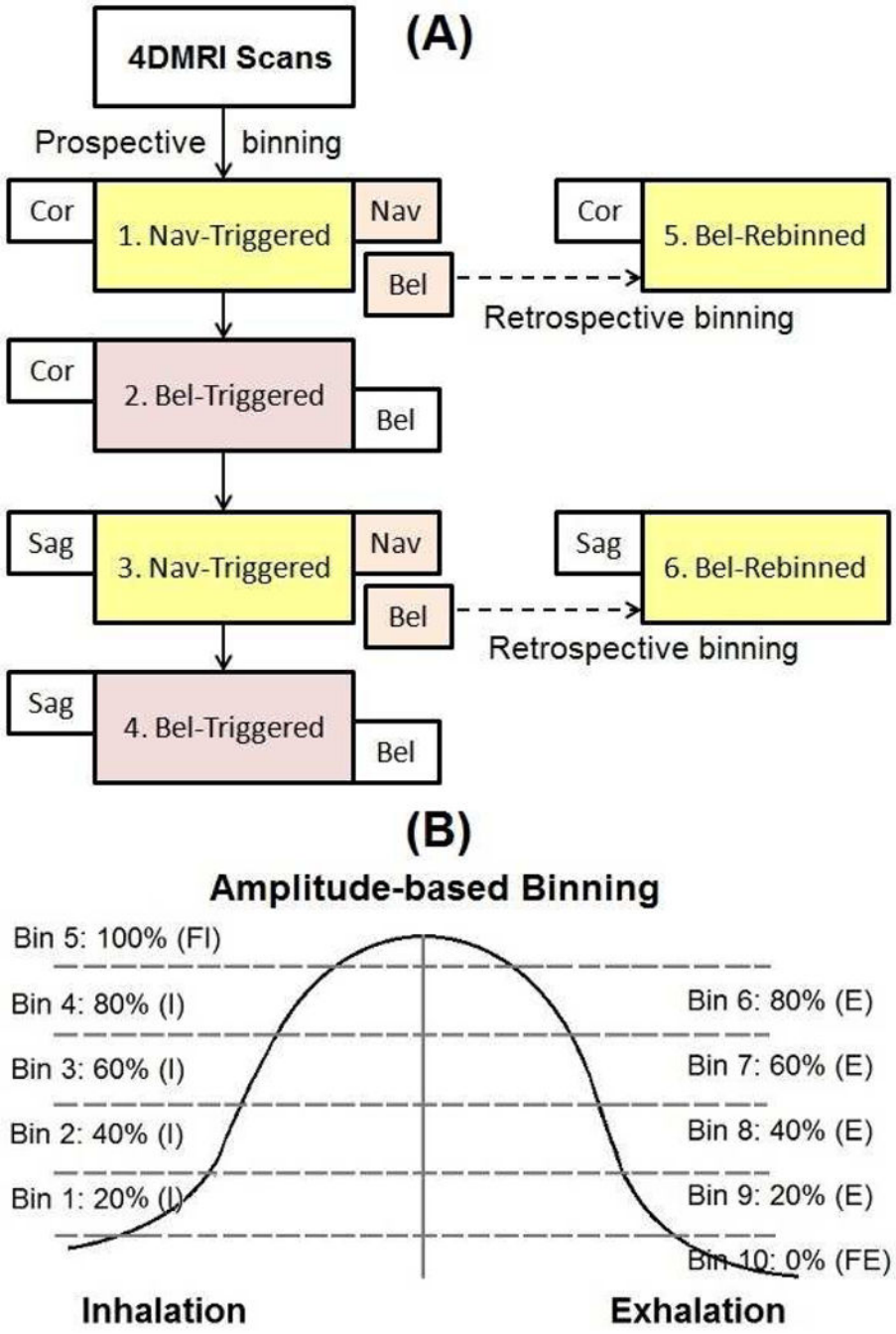

Figure 1.

4DMRI image acquisition work flow (A) and amplitude binning schematic (B). Four sets of prospective 4DMRI acquisition using navigator or bellows triggers were acquired and two sets of bellows-rebinned 4DMRI images using concurrent bellows signal were reconstructed.

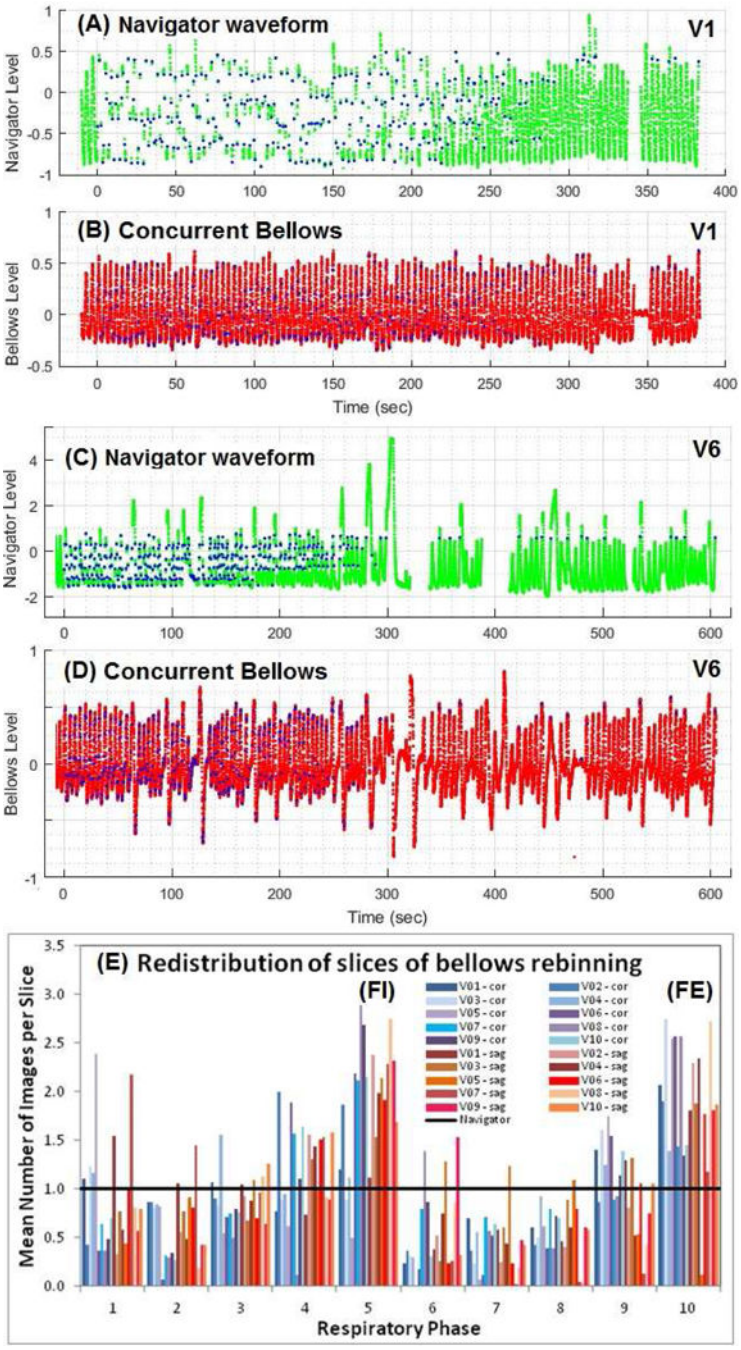

Figure 2.

Two concurrent pairs of navigator and bellows waveforms of a regular (V1:A&B) and an irregular (V6:C&D) breather. The blue dots in waveforms (A&C) are triggers for acquisition with 10s training period at the beginning, ~0.5s gaps during image acquisition, and ~20s gaps for patient instructions near the end. The blue dots in B&D are mapped from A&C based on time synchronization. The re-binning of navigator-triggered images makes the even slice distribution in navigator bins (black line) become uneven distribution in the bellows bins (E).

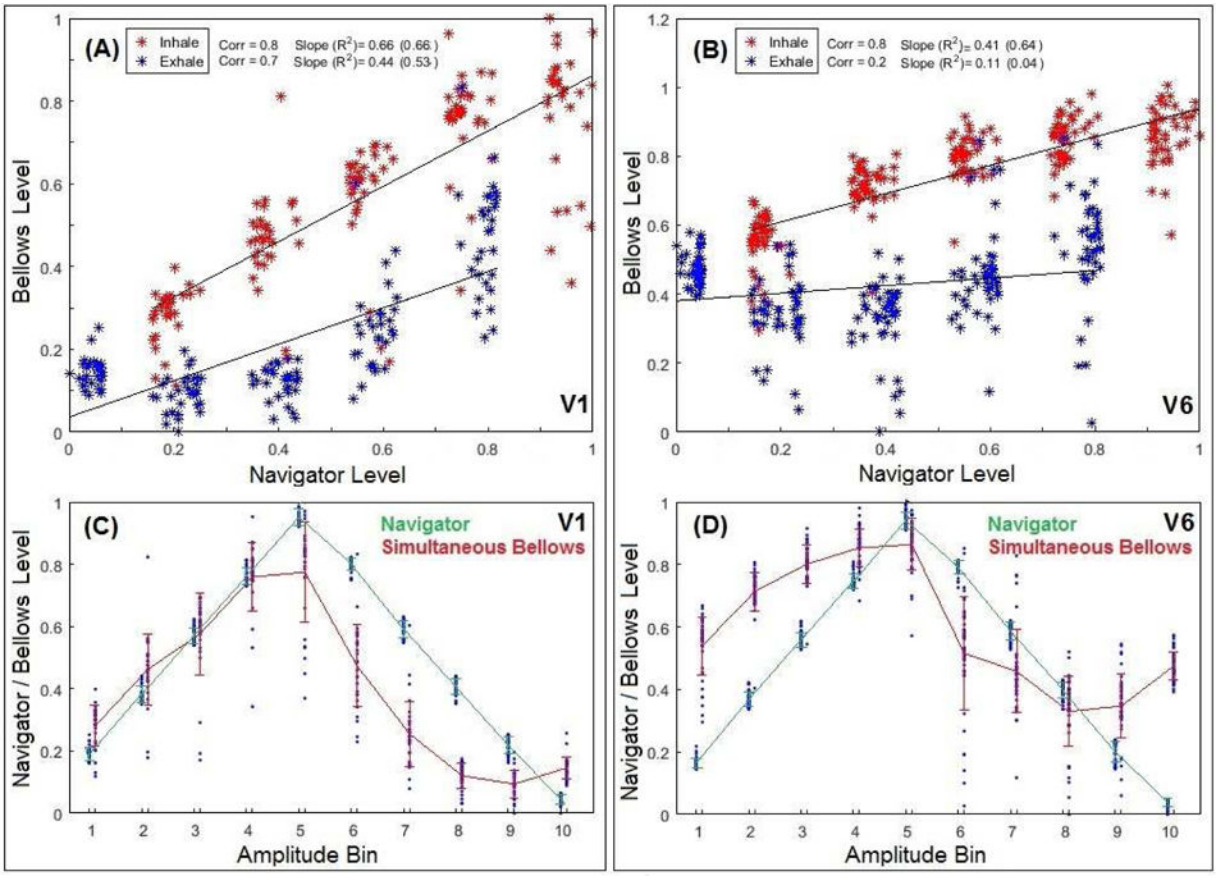

Figure 3.

Plots of concurrent navigator vs. bellows in two subjects (Volunteer 1:A&C and Volunteer 6:B&D). In A&B, acquisition points are binned in navigator amplitude level (X) and bellows amplitude level (Y). The evenly-distributed and separated navigator bins become spread and overlapping in bellows bins. The inhalation (red) and exhalation (blue) processes do not overlap in bellows level. In C&D, overlays of amplitude bin (X) vs. respiratory level (Y) for navigator and bellows. A phase shift is observed between the navigator-binned and bellows-binned waveforms.

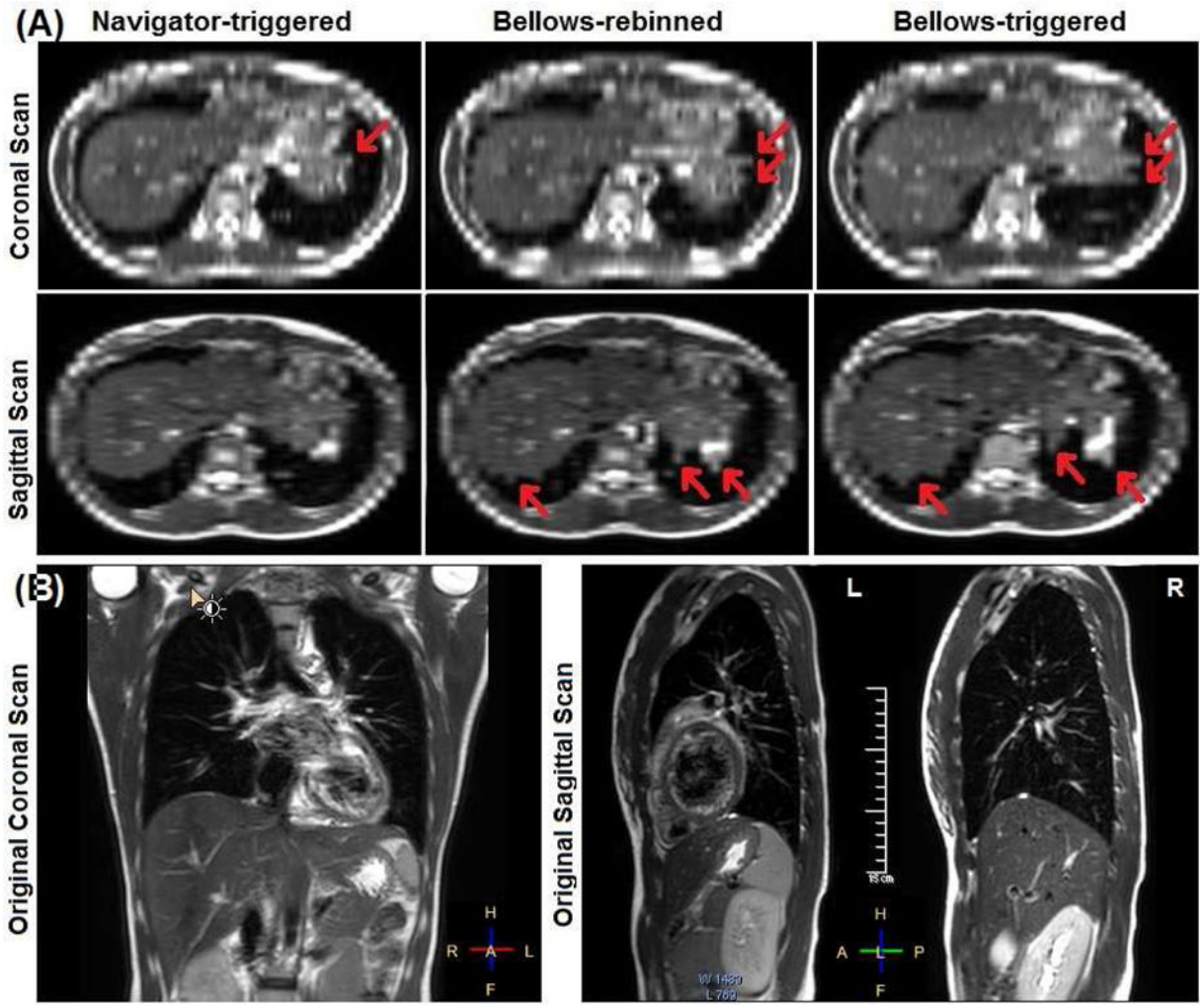

Figure 4.

Illustration of binning artifacts of navigator-triggered, bellows-rebinned (concurrent), and bellows-triggered (consecutive) 4DMRI images (volunteer 6) (A). The axial views are re-sliced from the coronal or sagittal scan images (B). The right diaphragm dome appears smooth in navigator-triggered 4DMRI, while both sets of bellow-based 4DMRI contain similar motion artifacts with irregular edges (red arrows).

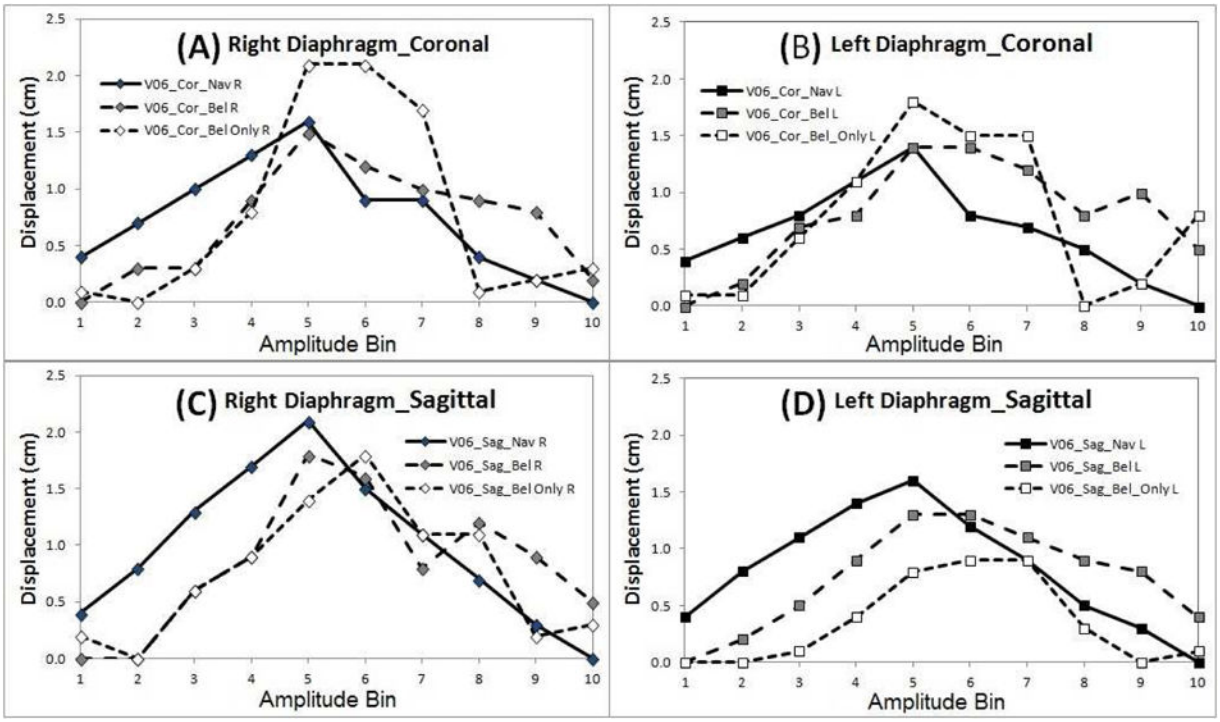

Figure 5.

Motion trajectories of two diaphragm domes in all 4DMRI images (volunteer 6) with bin shifts. Each sub-figure contains three trajectories from navigator-triggered scans (solid line), bellows-rebinned scans (dash line), and bellows-triggered consecutive scans (dot line).

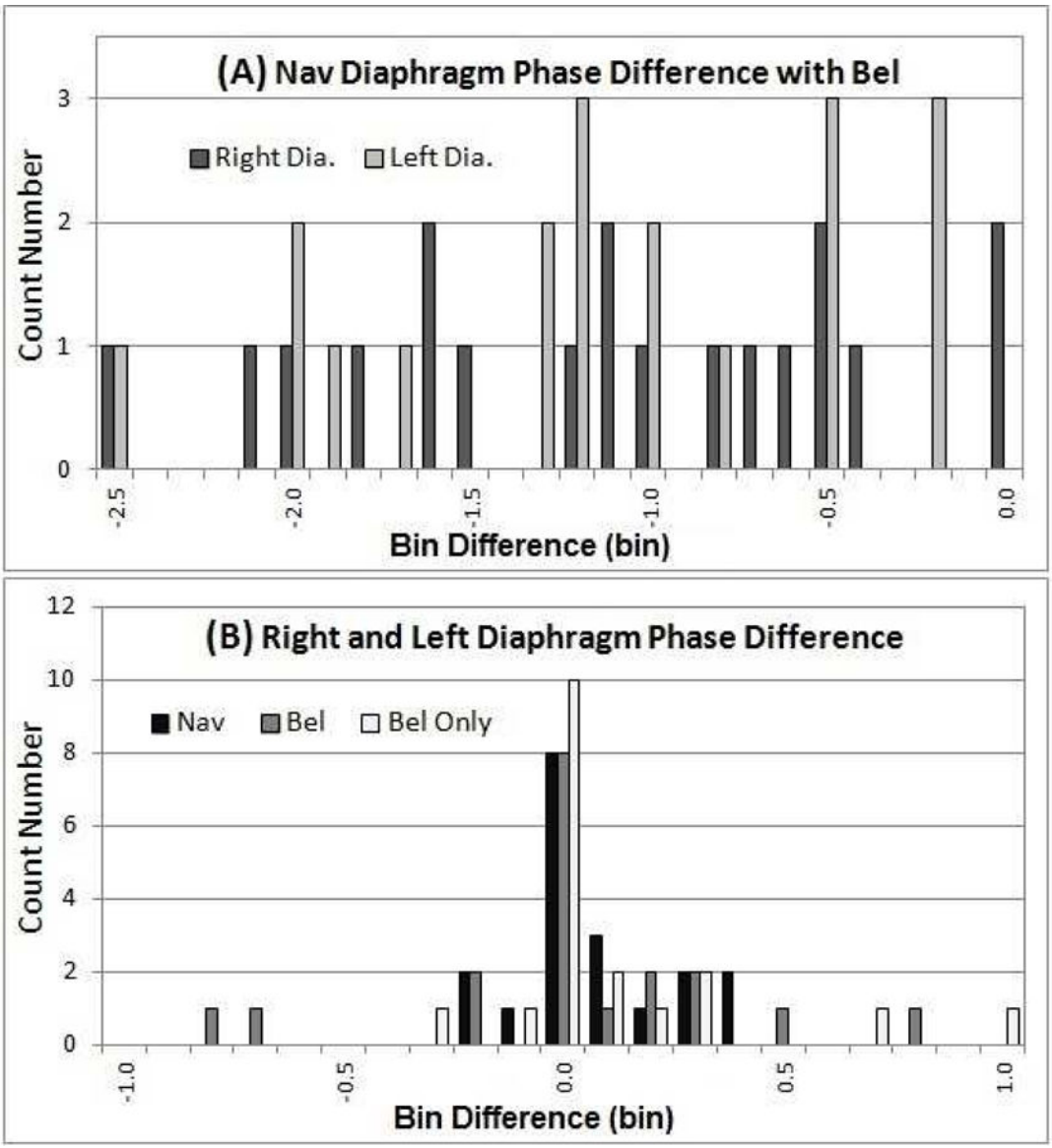

Figure 6.

Respiratory bin-shift histograms between navigator-triggered and bellows-rebinned 4DMRI images (A) and between the right and left diaphragms (B). Bellows is systematically lagging from the navigator by 0–2.5 bins (A) and bin shifts (<1) of the left-right diaphragm is random (B).

Table I

Correlation coefficient (corr) and linear slope between the navigator and bellows signal during inhalation and exhalation processes in coronal (C) and sagittal (S) scans.

Volunteer	Scan	Inhalation		Exhalation		Scan	Inhalation		Exhalation	
		Corr	Slope	Corr	Slope		Corr	Slope	Corr	Slope
1	C	0.81	0.67	0.73	0.44	S	0.67	0.49	0.66	0.39
2	C	0.82	0.42	0.37	0.27	S	0.66	0.25	−0.19	−0.11
3	C	0.91	0.80	0.64	0.27	S	0.92	0.62	0.81	0.43
4	C	0.16	0.10	0.19	0.11	S	0.18	0.13	−0.11	−0.07
5	C	0.45	0.42	0.25	0.10	S	−0.27	−0.20	0.48	0.36
6	C	0.77	0.28	0.50	0.22	S	0.81	0.41	0.21	0.11
7	C	0.46	0.20	0.61	0.43	S	−0.03	−0.02	−0.72	−0.33
8	C	−0.59	−0.29	−0.40	−0.23	S	0.44	0.18	−0.71	−0.43
9	C	0.43	0.21	0.26	0.17	S	0.15	0.08	−0.14	−0.10
10	C	0.64	0.31	0.38	0.21	S	0.54	0.28	0.27	0.16
Average		0.60	0.31	0.43	0.20		0.47	0.22	0.43	0.04
St. Dev.		0.23		0.18			0.30		0.28	

Table II

4DMRI scan time (minutes) and orientation in four primary prospective scans using navigator (Nav) or bellows (Bel) to trigger image acquisition.

Subject	Sex	Coronal Scan					Sagittal Scan				
		Scan Time (min)				Slice#	Scan Time (min)				Slice#
		Nav	95%#	Bel	95%#		Nav	95%#	Bel	95%#	
V01	F	6.5	4.8	6.3	5.5	30	12.1	7.1	6.7	5.7	52
V02	M	6.9	6.0	5.7	5.0	30	9.7	7.5	7.0	5.2	52
V03	M	9.4	8.2	6.1	5.4	35	9.6	6.9	7.4	6.3	57
V04	M	14.7	11.7	7.4	6.5	38	14.1	12.4	8.7	7.0	50
V05	F	8.8*	5.2	4.6	4.1	28	16.1*	14.1	5.4	4.7	43
V06	F	5.3	4.7	6.3	4.9	28	10.2	4.8	6.9	4.8	43
V07	M	8.2	7.0	5.2	4.2	28	9.6	8.5	7.0	4.9	47
V08	F	6.5	5.4	5.8	5.1	28	11.5	9.5	5.5	4.7	47
V09	F	9.7	8.2	9.7	4.9	29	11.6	9.7	7.7	5.5	47
V10	M	11.1	9.7	8.7	7.1	33	13.9	9.8	8.5	6.5	53
Mean		8.7	7.1	6.6	5.3	30.7	11.4	9.0	7.1	5.5	49.1
St Dev		2.9	2.3	1.6	0.9	3.5	1.8	2.7	1.1	0.8	4.5

#This means 95% of slices for 4DMRI has been acquired

*These volunteers breathe with a baseline drift, resulting in 3–5 slices at full inhalation phases not being collected due to the breathing irregularity and scanner time limit.